

Original Article

# Mass Spectrometry Imaging and Structural Analysis of Lipids Directly on Tissue Specimens by Using a Spiral Orbit Type Tandem Time-of-Flight Mass Spectrometer, SpiralTOF-TOF

Takaya Satoh,<sup>\*,1</sup> Ayumi Kubo,<sup>1</sup> Shuichi Shimma,<sup>2</sup> and Michisato Toyoda<sup>3</sup>

<sup>1</sup>JEOL Ltd., Akishima, Tokyo, Japan

<sup>2</sup>Division of Integrative Omics and Bioinformatics, National Cancer Center Research Institute, Chuo-ku, Tokyo, Japan

<sup>3</sup>Project Research Center for Fundamental Sciences, Graduate School of Science, Osaka University, Toyonaka, Osaka, Japan

In this paper, we report the use of mass spectrometry imaging and structural analysis of lipids directly on a tissue specimen, carried out by means of matrix-assisted laser desorption/ionization tandem time-of-flight mass spectrometry, using a combination of spiral orbit-type and reflectron-type time-of-flight mass spectrometers. The most intense peak observed in the mass spectrum from a brain tissue specimen was confirmed as phosphatidylcholine (34:1) [M+K]<sup>+</sup>, using tandem mass spectrometry. The charge remote fragmentation channels, which are characteristically observed using high-energy collision-induced dissociation, contributed significantly to this confirmation. Accurate mass analysis was further facilitated by mass correction using the confirmed peak. In mass spectrometry imaging, the high resolving power of our system could separate doublet peak of less than 0.1 u difference, which would otherwise be problematic when using a low-resolution reflectron type time-of-flight mass spectrometer. Two compounds, observed at *m/z* 848.56 and 848.65, were found to be located in complementary positions on a brain tissue specimen. These results demonstrate the importance of a high-performance tandem time-of-flight mass spectrometer for mass spectrometry imaging and analysis of observed compounds, to allow distinction between biological molecules.

**Keywords:** high-energy collision-induced dissociation, high-resolution precursor-ion selectivity, mass spectrometry imaging, time-of-flight mass spectrometer

(Received July 30, 2012; Accepted October 23, 2012)

## INTRODUCTION

Mass spectrometry imaging (MSI) can be used for biological applications,<sup>1)</sup> to assess the distribution of proteins,<sup>2,3)</sup> peptides,<sup>2,3)</sup> lipids,<sup>4-6)</sup> drugs,<sup>7-9)</sup> and their metabolites<sup>10,11)</sup> in a tissue specimen. Time-of-flight secondary ion mass spectrometry (TOF-SIMS) and matrix-assisted laser/desorption ionization mass spectrometry (MALDI-MS) are the two main types of MSI available. The lateral resolution of TOF-SIMS is much higher than that of MALDI-MS; however, MALDI-MS is often used in MSI of a tissue specimen because of its capacity for soft ionization.

A MALDI ion source can be used in most types of mass spectrometers. Especially, time-of-flight (TOF) mass spectrometers provide greater sensitivity, because all of the generated ions can be analyzed. On the other hand, inhomogeneity in the sample surface and variation in the size of the crystal or the matrix compound creates flight-path variation at each laser irradiation point during TOF mass spectrometry, causing mass drift. This negatively affects mass resolution during MSI of a relatively wide region. However, the drift can be reduced by employing a TOF mass spectrometer with a relatively long flight-path. A multi-turn type,<sup>12-16)</sup> a multi-reflecting type<sup>17-20)</sup> or a spiral orbit type<sup>21-26)</sup> TOF mass spectrometers, which have longer flight-paths, are

more useful than the conventional reflectron type of TOF mass spectrometer in this situation. We have previously reported the development of a spiral orbit-type TOF mass spectrometer (SpiralTOF),<sup>25)</sup> which has a 17-m-long flight-path, based on a multi-turn type TOFMS 'MULTUM II'.<sup>16)</sup> We have also developed a tandem TOF mass spectrometer (SpiralTOF-TOF), which combined SpiralTOF with a reflectron-type TOF mass spectrometer using an offset parabolic reflectron.<sup>26)</sup>

One of the advantages of a tandem TOF mass spectrometer is its capacity for high-energy collision-induced dissociation (HE-CID). The analysis of charge remote fragmentation (CRF) that is inherent to HE-CID enables confirmation of the detailed structure of fatty acid residues in lipids.<sup>27,28)</sup> In a conventional MALDI-tandem TOF mass spectrometer, fragmentation channels of post-source decay (PSD), which occurred in field-free regions in the first linear TOF mass spectrometers, are also observed in the product ion spectrum. However, PSD also occurs in an ion mirror observed as baseline noise in product ion spectrum conceals the relatively low-intensity CRF channels. In our SpiralTOF-TOF, the HE-CID channels can be preferentially observed, because the electrostatic sector in first SpiralTOF can eliminate PSD ions.<sup>29-32)</sup>

Here, we report the first trial of MSI using a high performance SpiralTOF-TOF, and demonstrate advantages in an analysis of lipids directly on a tissue specimen. The variety of lipid structures in biological samples complicates mass spectra; however, the high mass resolution of SpiralTOF

\* Correspondence to: Takaya Satoh, JEOL Ltd., 3-1-2 Musashino, Akishima, Tokyo 196-8558, Japan, e-mail: taksatoh@jeol.co.jp

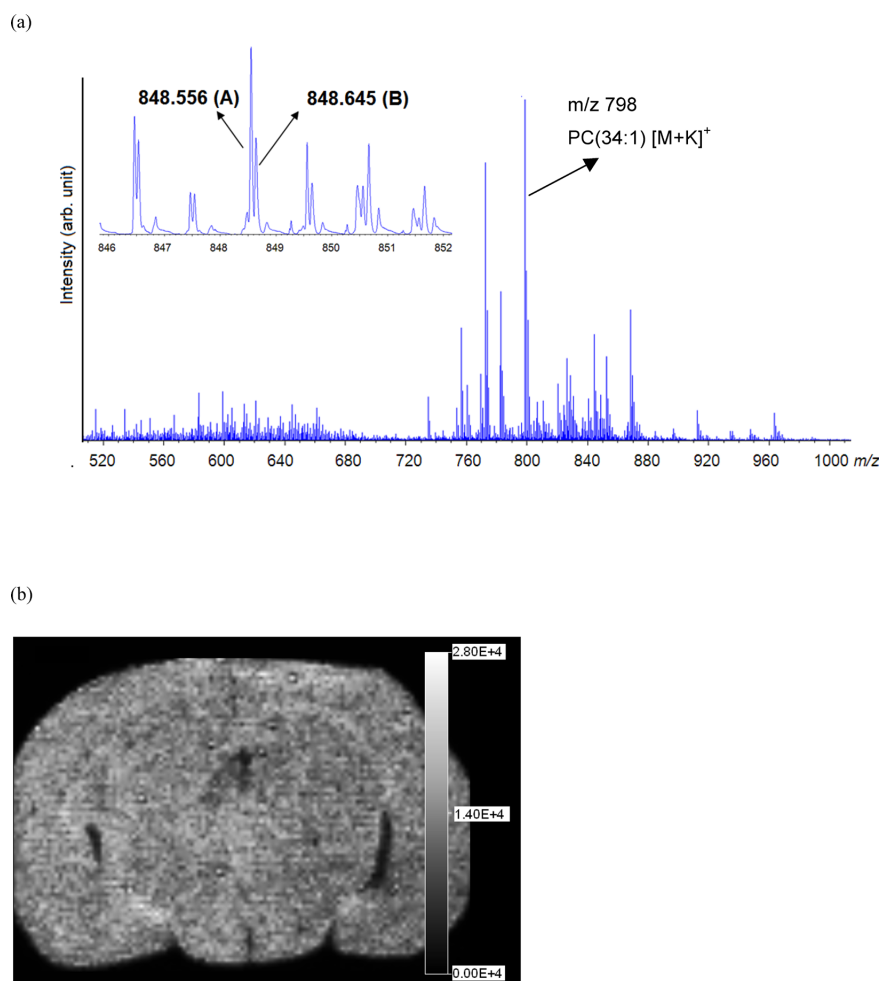


Fig. 1. (a) Averaged mass spectrum of 9676 mass spectra acquired during MSI. The spectrum at  $m/z$  846–852 is enlarged. (b) Mass image at  $m/z$  798 with a 0.1-u mass window. The compound is uniformly distributed throughout mouse brain tissue.

could resolve 0.1 u differences in doublet peaks, of which the mass spectrometry images then indicated a complementary distribution. Additionally, the presence of phosphatidylcholine (34:1) in tissue specimens was confirmed by a structural analysis using SpiralTOF-TOF. An accurate mass analysis was then possible after a mass correction, using the confirmed peak.

## METHODS

This study was approved by the Institutional Animal Experiments Committee and conducted in accordance with the guidelines of animal experimentation at Osaka University.

Six-week-old male C57BL/6J mice were anesthetized with isoflurane (Mylan Inc., PA, USA), sacrificed, and dissected. The brain block was immediately frozen in powdered dry ice to minimize degradation and was then maintained at  $-80^{\circ}\text{C}$ . The tissue sections were sliced into 10- $\mu\text{m}$ -thick sections using a cryostat and thaw-mounted on an indium-tin-oxide slide glass sample plate (HST Inc., NJ, USA). The samples were dehydrated in a vacuum chamber and the plate was mounted on a sample holder. As matrix compound, 2,5-dihydroxybenzoic acid (DHB) (Sigma-Aldrich, MO, USA) was dissolved in 100% methanol at a concentration of 30 mg/mL. A total amount of 2 mL of matrix solution was

sprayed on the individual tissue sections.

A standard of phosphatidylcholine (PC), 16:0/18:1 1-palmitoyl-2-oleoyl-*sn*-glycero-3-phosphocholine (PC [34:1]) (Polar Lipids, Inc., AL, USA) was used for comparing fragmentation channels observed directly from a tissue specimen; this standard was dissolved in tetrahydrofuran (THF) at a concentration of 100 nmol/mL.

DHB was dissolved in THF at a concentration of 20 mg/mL. The PC (34:1) and DHB solutions were mixed in a ratio of 1:1 (v/v); 0.5  $\mu\text{L}$  of this mixture was then deposited on a MALDI sample plate made of stainless steel using the dried-droplet method.

A SpiralTOF-TOF (JMS-S3000, JEOL Ltd., Akishima, Japan) was used for both MSI and MS/MS measurement. The instrument was equipped with a 349-nm Nd:YLF laser for MALDI. A laser repetition rate was 1-kHz. Mass spectra for MSI were acquired in a 9.52 $\times$ 6.56 mm region. The region was divided into 0.08-mm squares for each pixel, so that the MSI data consisted of 9,676 (=118 $\times$ 82) spectra. The mass spectrum in each pixel was acquired using 5,000 laser shots with a 1-kHz laser repetition rate. Because of a laser irradiation diameter, 0.02–0.03 mm, was smaller than a pixel size, a laser irradiation point was randomly changed within a pixel region in each 500 laser shots for 10 times. The total measurement time was 16 h. The raw data from JMS-S3000 were converted to imzML format<sup>33)</sup> and analyzed using biomap

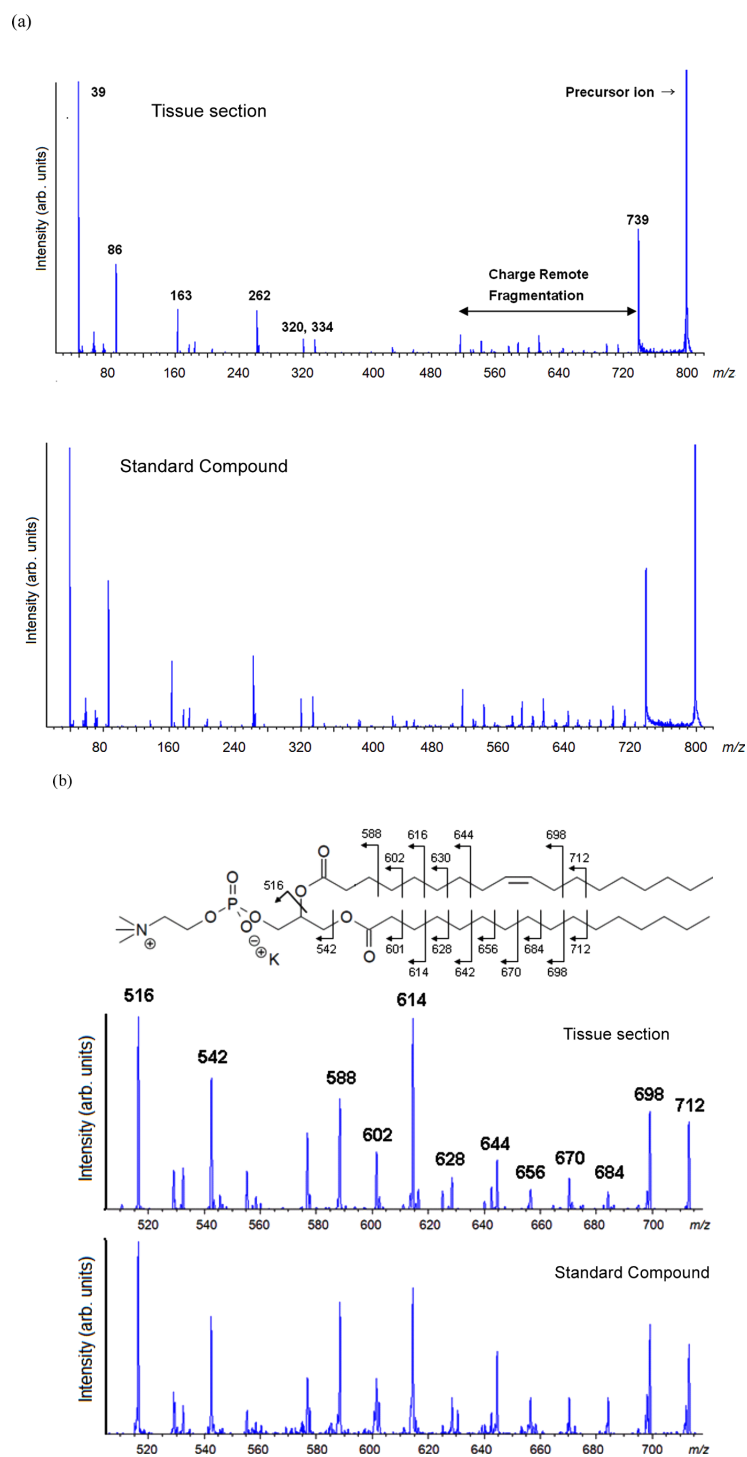


Fig. 2. (a) Comparison of product ion spectra at  $m/z$  798 from tissue section (upper) and standard PC (34:1)  $[M+K]^+$  (lower). (b) Enlarged spectra at  $m/z$  500–720, showing the charge remote fragmentation peaks.

Table 1. Differences between calculated and observed  $m/z$  values for phosphatidylcholine (PC) and phosphatidylethanolamine (PE) peaks observed in the averaged mass spectra after mass-correction using confirmed PC (34:1)  $[M+K]^+$ .

Compound	Ion type	Formula	Calculated $m/z$	Observed $m/z$	Error (ppm)
PC (32:0)	$[M+Na]^+$	$C_{40}H_{80}NO_8PNa^+$	756.5514	756.5493	-2.8
PC (32:0)	$[M+K]^+$	$C_{40}H_{80}NO_8PK^+$	772.5253	772.5242	-1.4
PC (34:1)	$[M+Na]^+$	$C_{42}H_{82}NO_8PNa^+$	782.5670	782.5660	-1.3
PE (38:4)	$[M+2K-H]^+$	$C_{43}H_{77}NO_8PK_2^+$	844.4656	844.4623	-3.9
PE (40:6)	$[M+2K-H]^+$	$C_{45}H_{77}NO_8PK_2^+$	868.4656	868.4612	-5.0

3.8.0.4 software.<sup>34)</sup>

## RESULTS AND DISCUSSION

The average of all mass spectra acquired in MSI is shown in Fig. 1(a); the enlarged averaged spectrum at  $m/z$  846–852 is also shown in Fig. 1(a). Lipid peaks were observed at  $m/z$  700–900. The most intense peak was at  $m/z$  798, which we deduced to be PC (34:1)  $[M+K]^+$  on the basis of a structure analysis using SpiralTOF-TOF (see below). The mass image at  $m/z$  798, described in a mass window of 0.1 u, is shown in Fig. 1(b). This compound was seen to distribute uniformly throughout the brain tissue section. Several doublet peaks were also observed in the averaged mass spectrum. For example, two peaks at  $m/z$  848.556 (A) and 848.645 (B), with a mass difference of 0.09 u, are shown in the enlarged spectrum. The high mass-resolving power of SpiralTOF, which is more than 25,000 (full width half maximum), could separate these doublet peaks clearly.

The information available from HE-CID product ion spectrum, which can sometimes determine positions of double bonds in fatty acid parts in lipids, was useful for structural analysis of lipids.<sup>27–29,31)</sup> Furthermore, comparison of product ion spectra from a tissue section and standard compound made confirmation more reliable. The product ion spectrum at  $m/z$  798 acquired directly from a tissue section (upper), and the product ion spectrum of the standard PC (34:1)  $[M+K]^+$  (bottom) are shown in Fig. 2(a). The precursor-ion selection window was  $\pm 0.7$  u at  $m/z$  798. Monoisotopic ions could be selected from among the precursor ions using the high precursor ion selectivity of SpiralTOF-TOF; the peaks shown in Fig. 2 are monoisotopic ions of the fragment ions generated. The major peaks at  $m/z$  39, 86, 163, 262, 320, 334, and 739 were observed in both mass spectra and were in good agreement. These peaks were corresponded to adduct ion and fragment ions derived from polar head group that could be also observed in a low-energy CID product ion spectrum. The enlarged mass spectra at  $m/z$  500–700 of Fig. 2(a) are shown in Fig. 2(b). The observed CRF peaks, which were characteristic peaks to HE-CID product ion spectrum, were indicative of fragmentation of fatty acid parts. They also agreed well between the two mass spectra. From these results,  $m/z$  798 was confirmed to correspond to PC (34:1)  $[M+K]^+$ .

In order to improve mass accuracy, the mass in Fig. 1(a) was corrected using only one peak at  $m/z$  798 should be coincided with calculated mass of PC (34:1)  $[M+K]^+$  ( $m/z$  798.5410). The chemical compositions of the five major peaks observed in the averaged mass spectrum were estimated using this more accurate mass analysis; these results are shown in Table 1. After mass correction, peaks could be assigned to phospholipids within a 5-ppm mass error.

The mass images of each peaks A and B in Fig. 1(a), which have only 0.09 u mass difference, were described in mass windows of 0.1 u in Figs. 3(a) and (b), respectively. The compounds representing peaks A and B were complementarily distributed in the white and gray matter, respectively, in each brain tissue section. The mass image at  $m/z$  848.600, in a mass window of 0.2 u, is also shown in Fig. 3(c) which represents a typical mass image obtained using a reflectron-type TOF mass spectrometer. In this image, an overlap of the images in Figs. 3(a) and (b) are shown, so that the

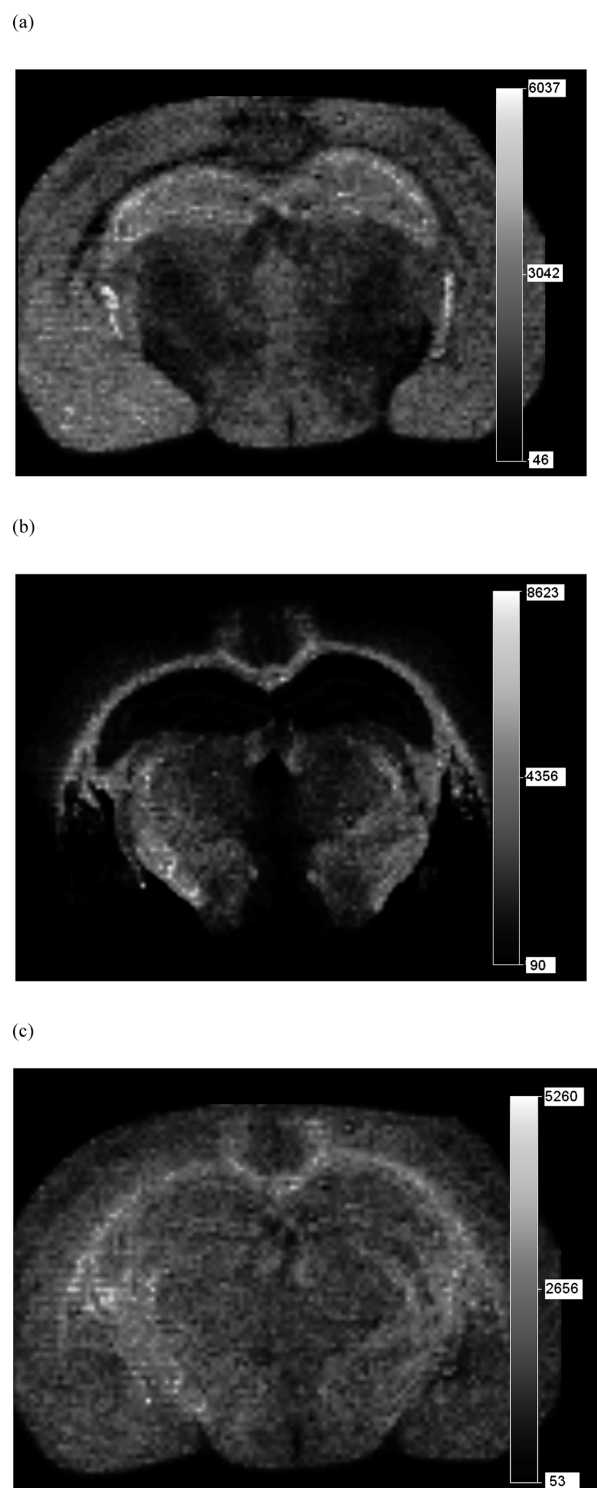


Fig. 3. The mass images at  $m/z$  848.556 and 848.645 in a mass window of 0.1 u are shown in (a) and (b). Two compounds observed at  $m/z$  848.556 and 848.645 were distributed in complementary locations. (c) The mass image in a mass window of 0.2 u, which includes  $m/z$  848.556 and 848.645. The overlapped image of (a) and (b) are shown.

inherent distribution of the compounds representing peaks A and B is lost.

The peaks A and B could not be isolated individually with the ion gate. Furthermore, it was difficult to accumulate product ion spectrum by laser irradiation where A and B were individually localized because of their low intensities.

We obtained product ion spectrum after selection of both peaks A and B simultaneously. Almost all fragment ions had difficulty in identification due to the complexities of spectrum. However, we found the intense peaks of potassium ions were generated from each precursor ions. From the adduct ion information  $[M+K]^+$  and accurate mass analysis, A and B were deduced to represent PC (38:4)  $[M+K]^+$  and galactosyl ceramide (C24h:1)  $[M+K]^+$ , respectively. Their distributions of PCs and galactosyl ceramides on tissue sections were agreed reasonably reported in ref. 35) shown by MS/MS analysis of major peaks. The advantage of using SpiralTOF-TOF is capability to draw selective mass images of minor doublet peaks, which were difficult to MS/MS separately.

## CONCLUSION

High-resolution mass spectrometry is an effective tool in MSI, however, itself does not allow compounds estimation of separated peaks. In spite of a high mass resolution, several dozen ppm ambiguities can be hidden in the  $m/z$  values of mass spectrum peaks. Improving the mass accuracy by mass correction, using peak confirmation by SpiralTOF-TOF, is therefore useful. Moreover, the high precursor-ion selectivity and the capacity for preferential observation of HE-CID fragmentation channels of SpiralTOF-TOF are particularly useful for confirming the structure of lipids.

## Acknowledgments

Authors thank Mr. N. Moriguchi, Assistant Professor Dr. H. Hazama and Professor Dr. K. Awazu for providing mouse brain tissue specimens.

## REFERENCES

- J. H. Jungmann, R. M. Heeren. Emerging technologies in mass spectrometry imaging. *J. Proteomics* 24 March 2012.
- R. M. Caprioli, T. B. Farmer, J. Gile. Molecular imaging of biological samples: Localization of peptides and proteins using MALDI-TOF MS. *Anal. Chem.* 69: 4751–4760, 1997.
- P. Chaurand. Imaging mass spectrometry of thin tissue sections: A decade of collective efforts. *J. Proteomics*. Available online 14 April 2012.
- Y. Sugiura, S. Shimma, Y. Konishi, M. K. Yamada, M. Setou. Imaging mass spectrometry technology and application on ganglioside study; Visualization of age-dependent accumulation of C20-ganglioside molecular species in the mouse hippocampus. *PLoS ONE* 3: e3232, 2008.
- S. Shimma, Y. Sugiura, T. Hayasaka, N. Zaima, M. Matsumoto, M. Setou. Mass imaging and identification of biomolecules with MALDI-QIT-TOF-based system. *Anal. Chem.* 80: 878–885, 2008.
- B. Colsch, S. N. Jackson, S. Dutta, A. S. Woods. Molecular microscopy of brain gangliosides: Illustrating their distribution in hippocampal cell layers. *ACS Chem. Neurosci.* 2: 213–222, 2011.
- B. Prideaux, V. Dartois, D. Staab, D. M. Weiner, A. Goh, L. E. Via, C. E. Barry 3rd, M. Stoeckli. High-sensitivity MALDI-MRM-MS imaging of moxifloxacin distribution in tuberculosis-infected rabbit lungs and granulomatous lesions. *Anal. Chem.* 83: 2112–2118, 2011.
- B. Prideaux, D. Staab, M. Stoeckli. Applications of MALDI-MSI to pharmaceutical research. *Methods Mol. Biol.* 656: 405–413, 2010.
- G. Hopfgartner, E. Varesio, M. Stoeckli. Matrix-assisted laser desorption/ionization mass spectrometry imaging of complete rat sections using a triple quadrupole linear ion trap. *Rapid Commun. Mass Spectrom.* 23: 733–736, 2009.
- Y. Sugiura, N. Zaima, M. Setou, S. Ito, I. Yao. Visualization of acetylcholine distribution in central nervous system tissue sections by tandem imaging mass spectrometry. *Anal. Bioanal. Chem.* 403: 1851–1861, 2012.
- Y. Sugiura, R. Taguchi, M. Setou. Visualization of spatiotemporal energy dynamics of hippocampal neurons by mass spectrometry during a kainate-induced seizure. *PLoS ONE* 6: e17952, 2011.
- W. P. Poschenrieder. Multiple-focusing time of flight mass spectrometers part II. TOFMS with equal energy acceleration. *Int. J. Mass Spectrom. Ion Phys.* 6: 357–373, 1972.
- T. Sakurai, H. Nakabushi, T. Hiasa, K. Okanishi. A new multi-passage time-of-flight mass spectrometer at JAIST. *Nucl. Instrum. Methods A* 427: 182–186, 1999.
- M. Toyoda, D. Okumura, S. Yamaguchi, M. Ishihara, I. Katakuse, T. Matsuo. Development of a multi-turn time-of-flight mass spectrometer 'MULTUM Linear plus.' *J. Mass Spectrom. Soc. Jpn.* 48: 312–317, 2000.
- D. Okumura, M. Toyoda, M. Ishihara, I. Katakuse. A simple multi-turn time of flight mass spectrometer 'MULTUM II.' *J. Mass Spectrom. Soc. Jpn.* 51: 349–353, 2003.
- M. Toyoda. Development of multi-turn time-of-flight mass spectrometers and their applications. *Eur. J. Mass Spectrom. (Chichester, Eng.)* 16: 397–406, 2010.
- H. Wollnik, M. Przewloka. Time-of-flight mass spectrometers with multiply reflected ion trajectories. *Int. J. Mass Spectrom. Ion Process.* 96: 267–273, 1990.
- H. Wollnik, A. Casares. An energy-isochronous multi-pass time-of-flight mass spectrometer consisting of two coaxial electrostatic mirrors. *Int. J. Mass Spectrom.* 227: 217–222, 2003.
- A. Verentchikov, M. Yavor, Y. Hasin, M. Gavrik. Multireflection planar time-of-flight mass analyzer. I: An analyzer for a parallel tandem spectrometer. *Tech. Phys.* 50: 73–81, 2005.
- M. Yavor, A. Verentchikov, J. Hasin, B. Kozlov, M. Gavrik, A. Trufanov. Planar multi-reflecting time-of-flight mass analyzer with a jig-saw ion path. *Physics Procedia* 1: 391–400, 2008.
- J. M. B. Bakker. A double-focusing design for time-of-flight mass spectrometers. *Int. J. Mass Spectrom. Ion Phys.* 6: 291–295, 1971.
- J. M. B. Bakker, D. A. Freer, J. F. J. Todd. Preliminary Studies on a New Time-Focusing Time-of-Flight Mass Spectrometer. in *Dynamic Mass Spectrometer Vol. 6* (Ed: D. Price and J. F. J. Todd), Hyden & Son, London, 1981, pp. 91–110.
- H. Matsuda. Spiral orbit time of flight mass spectrometer. *J. Mass Spectrom. Soc. Jpn.* 48: 303–305, 2000.
- H. Matsuda. Improvement of a TOF mass spectrometer with helical ion trajectory. *J. Mass Spectrom. Soc. Jpn.* 49: 227–228, 2001.
- T. Satoh, T. Sato, J. Tamura. Development of a high-performance MALDI-TOF mass spectrometer utilizing a spiral ion trajectory. *J. Am. Soc. Mass Spectrom.* 18: 1318–1323, 2007.
- T. Satoh, T. Sato, A. Kubo, J. Tamura. Tandem time-of-flight mass spectrometer with high precursor ion selectivity employing spiral ion trajectory and improved offset parabolic reflectron. *J. Am. Soc. Mass Spectrom.* 22: 797–803, 2011.
- M. L. Gross. Charge-remote fragmentations: Method, mechanism and applications. *Int. J. Mass Spectrom. Ion Process.* 118/119: 137–165, 1992.
- S. Trimpin, D. E. Clemmer, C. N. McEwen. Charge-remote fragmentation of lithiated fatty acids on a TOF-TOF instrument using matrix-ionization. *J. Am. Soc. Mass Spectrom.* 18: 1967–1972, 2007.
- S. Shimma, H. Nagao, M. Toyoda. Charge-remote fragmentation of phospholipids in a multi-turn tandem time-of-flight mass spectrometer "MULTUM-TOF/TOF." *J. Mass Spectrom. Soc. Jpn.* 55: 343–351, 2007. (in Japanese)
- S. Shimma, H. Nagao, A. E. Giannakopoulos, S. Hayakawa, K. Awazu, M. Toyoda. High-energy collision-induced dissociation

- of phosphopeptides using a multi-turn tandem time-of-flight mass spectrometer 'MULTUM-TOF/TOF.' *J. Mass Spectrom.* 43: 535–537, 2008.
- 31) S. Shimma, A. Kubo, T. Satoh, M. Toyoda. Detailed structural analysis of lipids directly on tissue specimens using a MALDI-SpiralTOF-Reflectron TOF mass spectrometer. *PLoS ONE* 7: e37107, 2012.
- 32) A. Kubo, T. Satoh, Y. Itoh, M. Hashimoto, J. Tamura, R. B. Cody. Structural analysis of triacylglycerols by using a MALDI-TOF/TOF system with monoisotopic precursor selection, accepted to *J. Am. Soc. Mass Spectrom.*
- 33) [http://www.maldi-msi.org/index.php?option=com\\_content&view=article&id=188&Itemid=63](http://www.maldi-msi.org/index.php?option=com_content&view=article&id=188&Itemid=63)
- 34) [http://www.maldi-msi.org/index.php?option=com\\_content&task=view&id=14&Itemid=39](http://www.maldi-msi.org/index.php?option=com_content&task=view&id=14&Itemid=39)
- 35) S. Taira, Y. Sugiura, S. Moritake, S. Shimma, Y. Ichiyanagi, M. Setou. Nanoparticle-assisted laser desorption/ionization based mass imaging with cellular resolution. *Anal. Chem.* 80: 4761–4766, 2008.